

**RESEARCH ARTICLE**

# Investigation of the effect of thermal insulation materials on packaging performance

Kaibao Wang | Liu Yang | Mariusz Kucharek

Department of Mechanical and Aerospace Engineering, University of Strathclyde, Glasgow, UK

**Correspondence**

Dr Liu Yang, Department of Mechanical and Aerospace Engineering, University of Strathclyde, 75 Montrose Street, Glasgow G1 1XJ, UK.

Email: l.yang@strath.ac.uk

**Funding information**

Tobermory Fish Company Ltd

**Abstract**

This investigation evaluates thermal insulation performance of a typical shipping container with different insulation materials. A mathematical model developed from our previous work was used to analyse the effect of packaging characteristics on insulative performance. A number of materials were employed as a liner to insulate a typical cardboard box, and the effect of these materials on package insulative performance was evaluated through experimental tests and the transient thermal model. The results showed that application of aluminium foil to the internal liner surface of polyethylene gave 46% increase in the package insulative performance compared with the original polyethylene-insulated packages. An improvement of 79% and 106% in insulative performance per unit liner thickness was obtained from packages insulated with a polyisocyanurate board and aerogel blanket compared with the polystyrene-insulated package. The results also indicated that temperature surrounding the package played a significant role in the maximum insulation time. Furthermore, an excellent agreement was obtained between the mathematical model and the experimental results across all packaging aspects studied in this work.

**KEYWORDS**

aerogel, insulation packaging design, packaging insulation performance, thermal insulation materials

## 1 | INTRODUCTION

Packages used to deliver temperature-sensitive products are typically insulated by a polyethylene (PE) or expanded polystyrene (EPS) liner. With an increasing market demand on long-haul transportation of fresh goods (e.g. foods and medicine), conventional insulation materials may no longer satisfy the requirement of temperature control during package delivery without significantly increasing the thickness of the liner. High performance insulation materials such as polyisocyanurate (PIR) and aerogel blankets (ABs) could potentially be utilised in packaging industry because of its extremely low thermal

conductivity. It also means that a similar thermal performance can be achieved with less lining materials of lower thermal conductivity and less amount of phase change materials (PCMs), which all contribute to package weight saving.

Market research shows that EPS and PE dominate the UK market share (over 60%) of materials used in insulating packaging production.<sup>1</sup> This is because of its low cost as well as its relatively good insulation performance. However, government regulations on these types of materials have limited the use as well as manufacturing. The alternative solution is natural materials such as natural wool and cellulose with a market share of 16%. It is more environmentally friendly, but

This is an open access article under the terms of the Creative Commons Attribution-NonCommercial-NoDerivs License, which permits use and distribution in any medium, provided the original work is properly cited, the use is non-commercial and no modifications or adaptations are made.

© 2020 The Authors. Packaging Technology and Science published by John Wiley & Sons Ltd

the manufacturing cost is higher than EPS and PE with similar insulation performance. Vacuum insulation panels (VIPs) as a recent advanced insulation material provide the best thermal insulation at high cost.

It is often time-consuming and more costly to design an insulative package through physical tests.<sup>2</sup> Therefore, it is beneficial to develop a predictive model for packaging design under consideration of key design parameters such as insulation materials, packaging geometry and surrounding environment. G. Burgess and J. Singh indicated that the interaction between the  $R$ -value and the wall thickness significantly influenced the thermal performance.<sup>3, 4</sup> S. Choi et al. has derived a mathematical model to calculate the heat penetration rate (HPR) across the package, and then, the model has been validated using an ice melt test. The effect of aluminium foil and variable outside temperature has also been discussed. It has been stated that in most cases, the effect of foil is maximized when the foil is applied to the inner surface of the package.<sup>5</sup> However, larger experimental errors have been obtained using the ice melt test. J. Terpak et al. has developed a mathematical model to investigate the time required for products to reach 32°C when considering heat transfer by conduction, convection and radiation individually and combined.<sup>6</sup> Despite this transient approach, simplified package geometry and construction is a limiting factor that can lead to a significant uncertainty. Nevertheless, the model showed clearly that a change of surface emissivity can influence the thermal radiation significantly and the change of insulation liner thickness results in substantial difference in conduction. Unfortunately, little experimental data were obtained to validate the transient model. D.M. Stubbs et al. indicated that the performance of packages is maximised when the product is surrounded by refrigerants using in-house software.<sup>7</sup> B. Margeirsson et al. investigated the temperature distribution within the package using computational fluid dynamics (CFD) and verified experimentally.<sup>8</sup> K. Valtysdittir et al. redesigned a standard rectangular EPS box by increasing the radius of the internal corner using CFD methods. A better thermal insulation performance was achieved.<sup>9</sup> G. Xie<sup>10</sup> and J. Xie<sup>11</sup> investigated the heat transfer mechanism of a corrugated sandwich structure using a finite element method, which proves that such design is beneficial for thermal performance.

In this work, we used a transient model developed in-house to assess insulation performance of passive insulated packages and compared modelling results with experimental measurement for a wide range of design parameters for a typical passive insulated package. In particular, high performance insulation materials such as PIR and AB were compared with other conventional materials in terms of their influence on packaging insulative performance.

## 2 | ANALYICAL MODELLING

A passively insulated package typically includes a container, whose walls may consist of single or multiple layers of insulating materials. In order to understand heat flow in the passively insulated package, an analytical model has been developed in-house and reported in detail

previously.<sup>1</sup> This computational model was achieved by combining steady state and transient models in a 2D geometry for a typical shipping container. In this model, the HPR of a multi-layered wall was first derived using the method in Choi and Burgess<sup>5</sup> and was subsequently validated by an ice melt test. The HPR is defined to be the amount of heat flowing into the package at a unit temperature difference across package walls. Thus, the relationship between the HPR and total thermal resistance,  $R_q$ , of the package can be described as:

$$R_q = \frac{1}{\text{HPR}} \quad (1)$$

The total thermal resistance was then used in an energy balance equation for the package subjected to a temperature gradient across the walls, and the solution of the energy balance equation describes the temperature change inside the package as a function of time:

$$T(t) = (T_i - T_e) e^{-\frac{t}{R_q(m_1 C_1 + m_2 C_2)}} + T_e \quad (2)$$

where,

$m_1$	=	Mass of the product in kilogrammes
$C_1$	=	Specific heat capacity of product in joules per kilogramme per kelvin
$m_2$	=	Mass of the coolants in kilogrammes
$C_2$	=	Specific heat capacity of coolants in joules per kilogramme per kelvin
$T_i$	=	Initial temperature of product in kelvin
$T_e$	=	Exterior surrounding temperature in kelvin
$t$	=	Time in seconds

Several assumptions have been applied to the model. Firstly, conduction is considered as a dominating mechanism for heat transfer in a perfectly closed package surrounded with negligible fluid displacement. Furthermore, it is assumed that there is no significant air gap between insulation materials and cardboard boxes, and temperature change of coolant and the transported product will change at the same rate with time. Finally, uniform temperature distribution is assumed at any given time for the coolant and the transported product in the package. The key input parameters for this model are package dimensions, thickness and thermal conductivity of an insulation liner, mass of coolants, material surface emissivity and surrounding temperature. All of these parameters can be varied within the model to predict the insulating performance of a packaging design.

In the present work, the package insulating performance was characterised by the maximum insulation time (MIT), which was defined as the time required for coolant temperature increase from  $-20^\circ\text{C}$  to  $5^\circ\text{C}$  as it has been proven by the previous research that  $5^\circ\text{C}$  tends to be an upper limit temperature for transportation of perishable goods (e.g. fish).<sup>12, 13</sup> When phase change materials (e.g. ice) are present inside the package, the latent heat of fusion of coolant must be

taken into account for the calculation of the MIT. During the phase change, the temperature was set to be constant in this work, and the amount of time required to complete the phase change was calculated when total heat flow reached the latent heat determined by the amount of coolant and its specific latent heat. Before and after the phase change, Equation 2 was used to determine the temperature changes inside the package. The total time associated with the sensible heat was obtained by implementing a 'for' loop function of Equation 2 in MATLAB to calculate the package internal temperature every second of time elapsed. Amounts of energy being added and total heat flow across packaging walls were also calculated by the model to identify the time when the phase change should commence and finish. As a result, a complete temperature–time profile before, during and after a coolant phase change was obtained for an insulated package, and the MIT was obtained at the temperature of 5°C.

### 3 | EXPERIMENTAL

#### 3.1 | Materials

Single corrugated cardboard boxes with dimensions  $25.6 \times 20.5 \times 21.2$  cm and a thickness of 2.68 mm were obtained from Packaging Now Ltd. PE liners and packaging-grade EPS liners (10–12 g/L) were purchased from an online store. Food catering aluminium foil was supplied by Kirkland. Kingspan TF70 PIR boards were supplied by Encon Insulation Ltd. An AB of 1 cm thickness was purchased from Aerogel UK Ltd. Mylar bags (PET film sandwiched by aluminium foil) were obtained from Fresherpack Ltd. Two 400-g Thermos ice packs (99.4% H<sub>2</sub>O) purchased from Miage Ltd were used

in order to keep the volume and shape of coolants constant throughout all experiments.

#### 3.2 | Measurement of maximum insulation time

Experiments were carried out with cardboard boxes fitted with pre-cut liners of different insulation materials as shown in Figure 1. Average thickness of the insulation materials is summarised in Table 1. Two layers of AB liners had to be used in order to achieve a insulation thickness similar to other insulation materials. The measurement of thermal insulation performance of the packages was carried out according to ASTM D3103-14. Lab environment was controlled at temperature of  $22^\circ\text{C} \pm 3^\circ\text{C}$  and relative humidity of  $50\% \pm 5\%$ . The coolants were preconditioned in a freezer with a temperature of  $-21^\circ\text{C}$  for 48 h before they were positioned inside the box as shown in Figure 2. A temperature sensor with accuracy of  $\pm 0.1^\circ\text{C}$  was used,

**TABLE 1** Measurement of thermal conductivity and thickness at 20°C

Material	Ave. thermal conductivity (megawatts per metre-kelvin)	Ave. thickness (millimetres)
Polyisocyanurate	$24.6 \pm 0.04$	$25.42 \pm 0.01$
Aerogel blanket	$16.2 \pm 0.02$	$9.42 \pm 0.02$
Polyethylene	$61.0 \pm 0.18$	$27.45 \pm 0.03$
Expanded polystyrene	$42.5 \pm 0.06$	$24.38 \pm 0.02$
Cardboard box	$43.9 \pm 0.46$	$2.68 \pm 0.00$

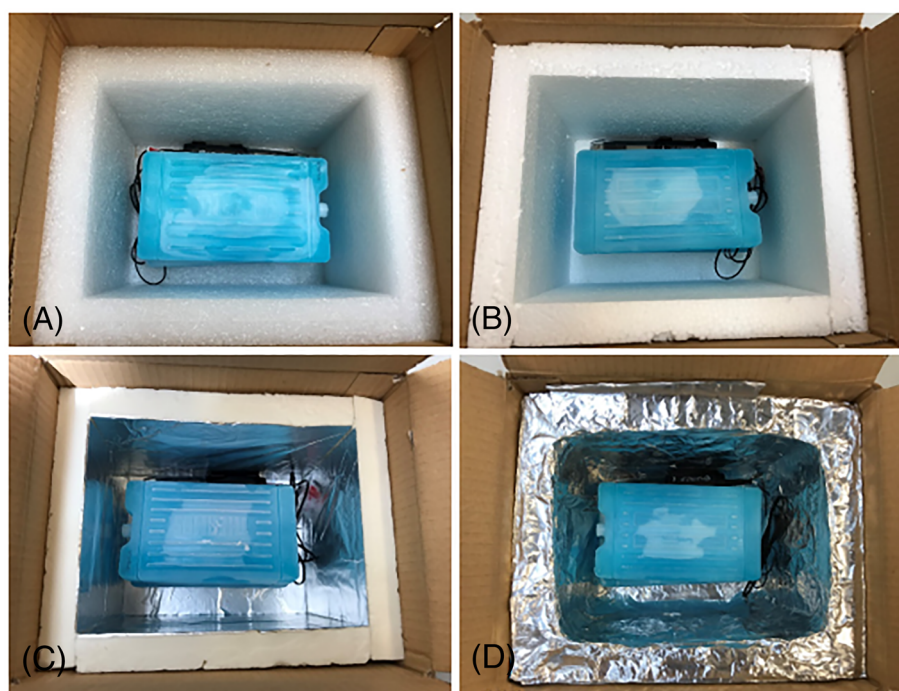


**FIGURE 1** Package prototype with various insulation lining materials including, A, polyethylene (PE); B, expanded polystyrene (EPS); C, polyisocyanurate (PIR) with aluminium foil; D, aerogel blanket with aluminium foil

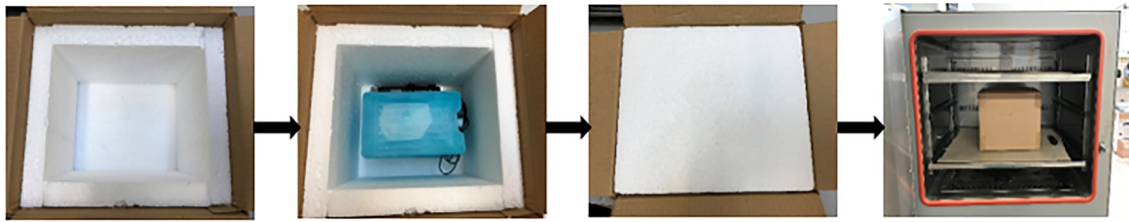


**FIGURE 2** Procedure of measurement of package insulation performance

and the sensor probe with a diameter of 0.4 cm and length of 2.5 cm was sandwiched between the two ice packs (the temperature variation of different sensor location was investigated in section 3.3 below) once the insulation lid was put on and the box was sealed. The package was then placed in an oven to initiate the MIT test. The oven was preheated to the desired temperature for 2 h before the package was put in the oven, and the temperature was monitored by an additional temperature sensor with an accuracy of  $\pm 0.5^\circ\text{C}$ . The basic operation procedure is demonstrated in Figure 2. All MIT measurements were repeated three times to obtain an average value.

### 3.3 | Positioning of temperature sensor

As coolant inside the package is the main temperature regulator in the passive insulated package, it is paramount to accurately measure its temperature change with elapsed time. Consequently, the time-temperature variation obtained with different sensor positioning was first examined to identify the temperature difference within the box as shown schematically in Figure 3. In Figure 3A, the temperature sensor is placed on top of the ice packs to measure the surface temperature of the ice pack. In Figure 3B, the temperature sensor is placed in between the ice packs to measure the bulk temperature of the ice pack. The PE insulated package was used in this case, and the MIT measurement was conducted at room temperature.

### 3.4 | Measurement of surface emissivity

Surface emissivity measurement was carried out according to the procedure described in Luo and Sun.<sup>14</sup> A sample was placed on a hot plate set at a constant temperature of  $50^\circ\text{C}$  in order to create more than at least  $10^\circ\text{C}$  difference than surrounding temperature as required in ASTM E1933-14. A thermocouple was used to detect

material surface temperature ( $T_{\text{obj}}$ ) as well as the surrounding air temperature ( $T_{\text{sur}}$ ). An infrared (IR) thermometer was used to detect surface temperature ( $T_{\text{obj}}$ ) when emissivity was set to 1. These measured temperatures were used to calculate surface emissivity ( $\epsilon$ ) of the sample by Equation 3.

$$\epsilon = \frac{[T_{\text{obj}}^4 - T_{\text{sur}}^4]}{[T_{\text{obj}}^4 - T_{\text{sur}}^4]} \quad (3)$$

Figure 4 shows the experimental setup for aluminium foil, PE and mylar film respectively. In order to validate the influence of inner surface emissivity on package performance, experiments were carried out by applying mylar film and aluminium foil on the same PE insulated package at surrounding temperature of  $40^\circ\text{C}$ .

### 3.5 | Measurement of thermal conductivity

The Netzsch Heat Flow Meter 436 with thickness gauge was used to measure the thermal conductivity and thickness of insulation materials accurately according to ASTM C518-17. The measurement was carried out at various temperatures, and a constant pressure load of 2 kPa was applied during all measurement.

## 4 | RESULTS AND DISCUSSION

### 4.1 | Effect of temperature measurement

Figure 5 shows a comparison of time-temperature profile obtained from a temperature sensor positioned on top of the ice packs (Figure 5A) and from a temperature sensor sandwiched between two ice packs (Figure 5B), respectively. It can be seen from Figure 5A that

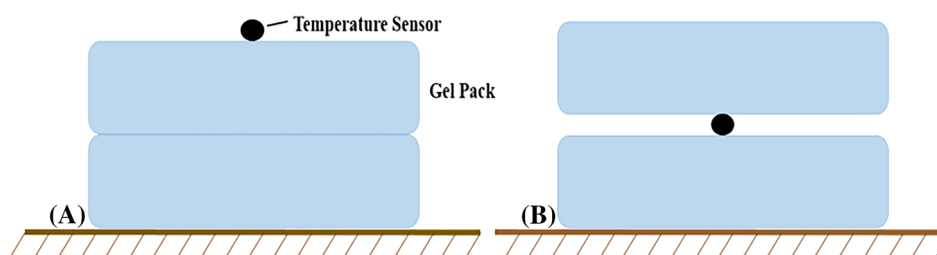


**FIGURE 3** Illustration of temperature sensor position with respect to the ice packs

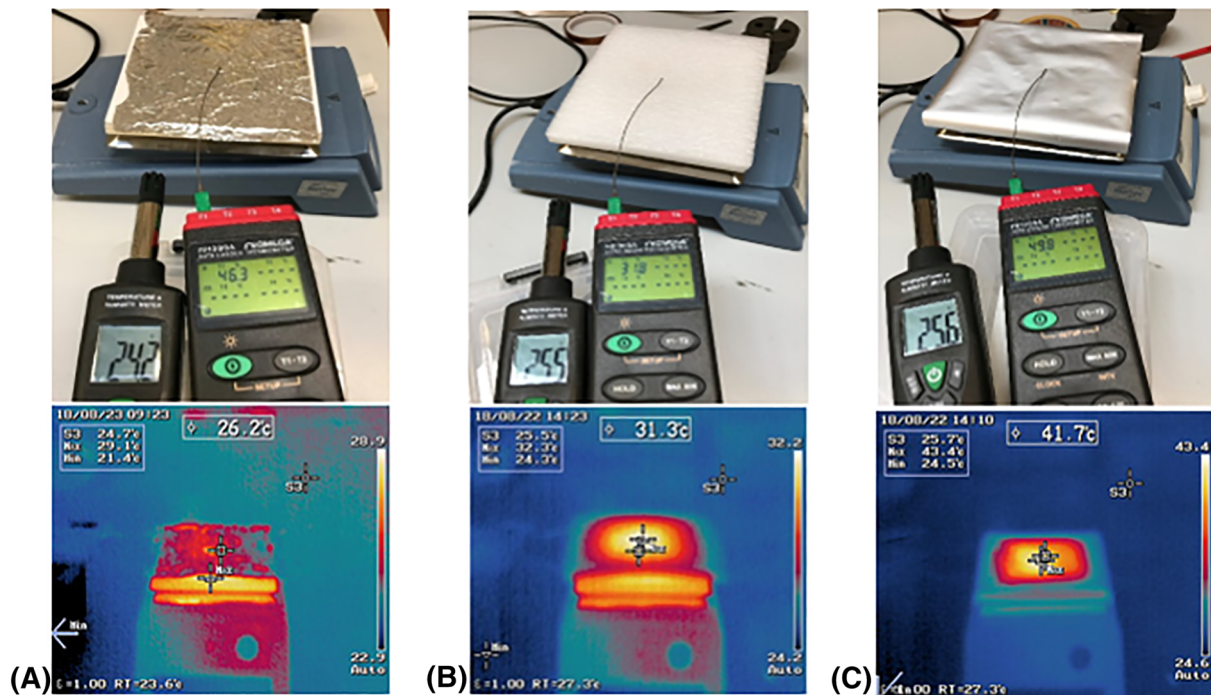
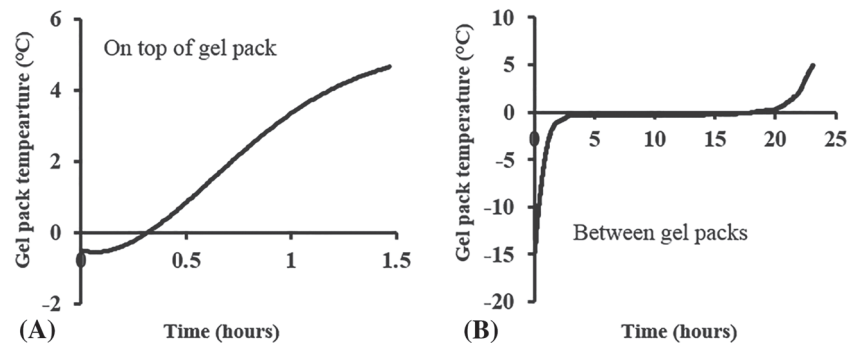


**FIGURE 4** Measurement of material surface emissivity including (a) aluminium (b) PE (c) mylar film

**FIGURE 5** Effect of temperature sensor position on the measurement of ice packs temperature as a function of time



surface temperature of the ice pack increased rapidly and continuously. As a result, the surface temperature reached 5°C in 1.5 h. On the contrary, when the sensor is sandwiched between the two ice packs, the phenomenon of latent heat is clearly illustrated as shown in Figure 5B. In Figure 5B, the temperature–time profile can be divided into three distinct stages. The first stage showed rapid temperature increase before it reached melting temperature of the ice packs. This was followed by a prolonged stage for ice melting with little temperature change in the container. Upon completion of this phase change, the temperature experienced another rapid increase towards the external temperature. It is obvious that the MIT is dominated by the second stage controlled by the PCM in the package.

For all future experiments, sensor position layout shown in Figure 3B will be adopted due to the following reasons. The results shown in Figure 5B clearly define three different stages of temperature–time behaviour that does not appear in Figure 5A. Figure 3B is more representative to how delivery product is

positioned with respect to ice packs. A temperature sensor is less affected by natural convection inside the package during the measurement.

#### 4.2 | Effect of surface emissivity on maximum insulation time

Figure 6 shows the results for the surface emissivity of different materials used in this work. It is well known that material with highly reflective surface such as aluminium foil and PIR composite foil have much lower emissivity value than rough and low reflective surface such as EPS and PE. It can also be seen from Figure 6 that the measured results for surface emissivity are in good agreement with the literature value.<sup>15</sup> However, this property is also affected by surface colour and topography. In this work, directly measured values were chosen for the model to evaluate the influence of emissivity on the

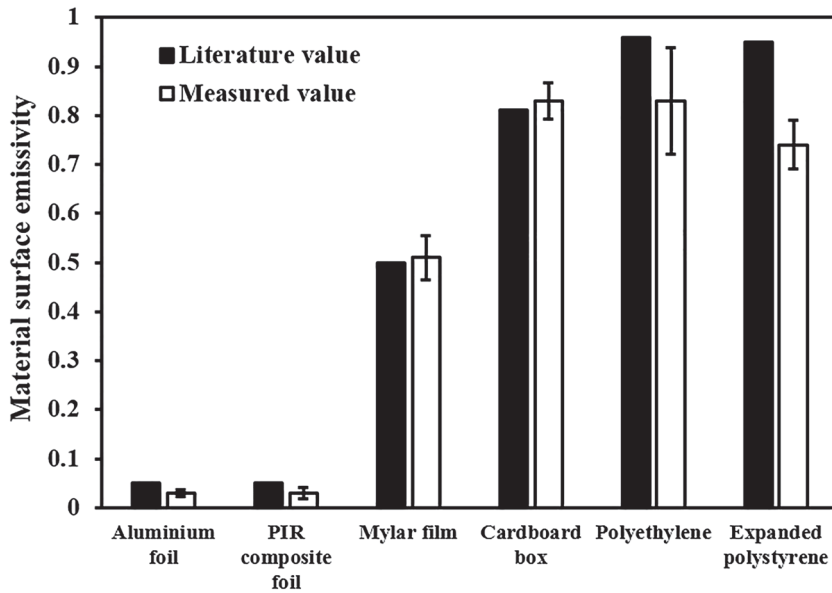


**FIGURE 6** Material surface emissivity comparison between literature and measured values

MIT in order to improve the accuracy of the results produced by the model.

The effect of internal surface emissivity on the MIT at surrounding temperature of 40°C is presented in Figure 7. It is indicated by the analytical model that as package internal surface emissivity value increases from 0.03 to 1, a reduction of almost 40% is expected to obtain from the MIT. Surface emissivity is the crucial factor in relation to radiation heat transfer as described by the Stefan–Boltzmann law. Increase in surface emissivity will lead to less reflected heat and an increase in the heat energy transfer through the container wall. It can also be seen from Figure 7 that a good agreement between the calculated and measured values is achieved with approximately 10% discrepancy. As a result, 46% increase in the MIT is obtained with aluminium foil applied on PE inner surface compared to the original PE insulated package. This agrees with the observation achieved in other study as well.<sup>6</sup>

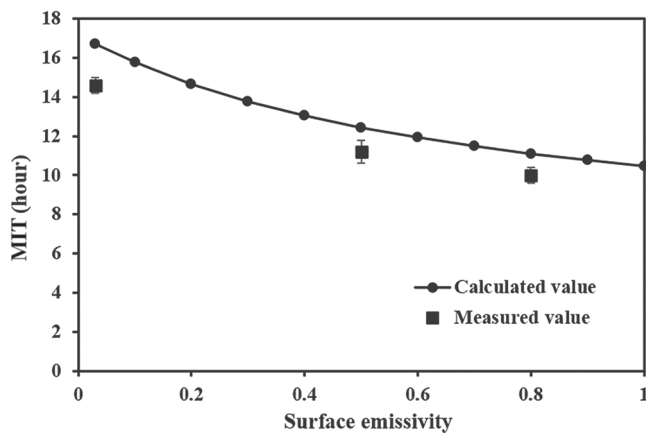


**FIGURE 7** Effect of internal surface emissivity on maximum insulation time at surrounding temperature of 40°C using PE insulated package. PIR, polyisocyanurate

### 4.3 | Effect of insulation materials on maximum insulation time

Figure 8 presents the calculated MIT as function of thermal conductivity of the insulation liner at surrounding temperature of 20°C. Thermal conductivity of insulation liner and external box is considered separately. When assessing the effect of thermal conductivity of insulation liner on the MIT, the thickness and thermal conductivity for external box remain constant. It can be seen from Figure 8 that the MIT tends to drop rapidly with the increase of wall thermal conductivity and the rate of MIT change decreases gradually as the wall conductivity increases. This trend continues until the MIT levels off and remain unaffected by the wall conductivity. It is well expected that the MIT will decrease as packaging walls become more thermally

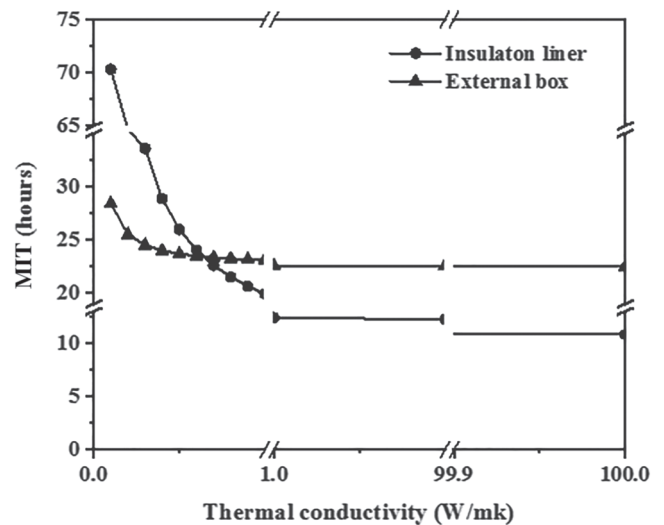
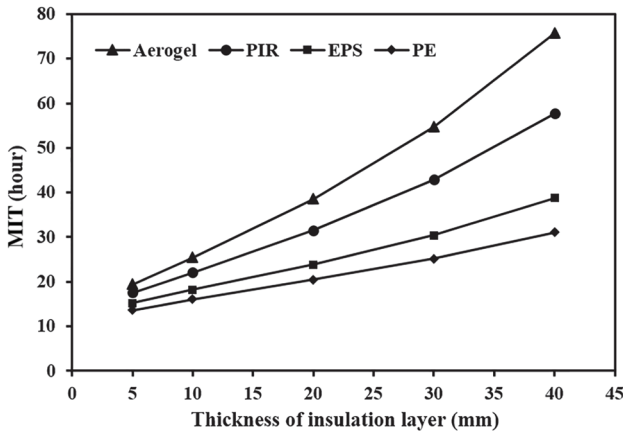


**FIGURE 8** Effect of thermal conductivity of insulation liner and external box on calculated maximum insulation time at surrounding temperature of 20°C

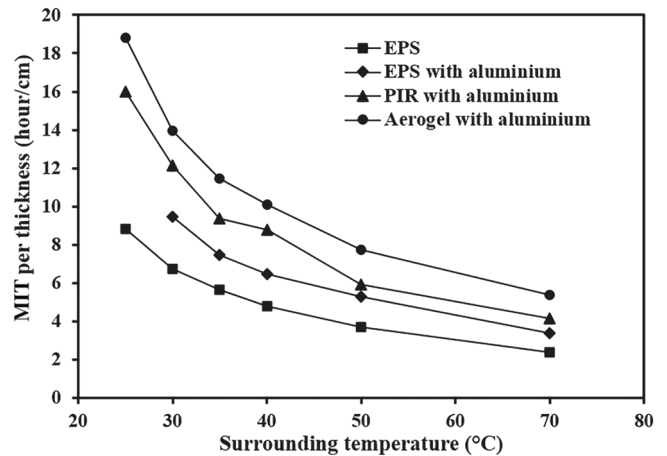
conductive. However, the overall behaviour of the MIT is affected by both wall thickness and thermal conductivity. Because cardbox thickness (2.68 mm) is significantly less than the PE liner thickness (27.45 mm), the effect of thermal conductivity on the MIT will be much less prominent for the cardbox than the insulation liner as shown in Figure 8. For a given wall thickness, its insulation effect will diminish as the wall becomes more and more heat conductive. It follows that the plateau in Figure 8 represents the MIT provided only by the cardbox/insulation liner when insulation liner/cardbox becomes very conductive.

Figure 9 shows the influence of insulation thickness on the MIT. It is obvious that the MIT increases as the insulation liner becomes thicker; however, in practice, liner thickness may be restricted either by dimensions of packages or cost. As mentioned previously, the MIT is affected by both the wall conductivity and thickness. This becomes evident when Equation 2 is rearranged into

$$t = -R_q * (C_{p1} * m_1 + C_{p2} * m_2) * \ln \left( \frac{T(t) - T_e}{T_i - T_e} \right) \quad (3)$$



**FIGURE 9** Effect of insulation thickness on calculated maximum insulation time for insulation material including aerogel blankets (ABs), polyisocyanurate (PIR), expanded polystyrene (EPS) and polyethylene (PE) at surrounding temperature of 20°C



**FIGURE 11** Comparison of calculated and measured maximum insulation time per unit thickness for packages insulated with different materials at surrounding temperature of 30°C

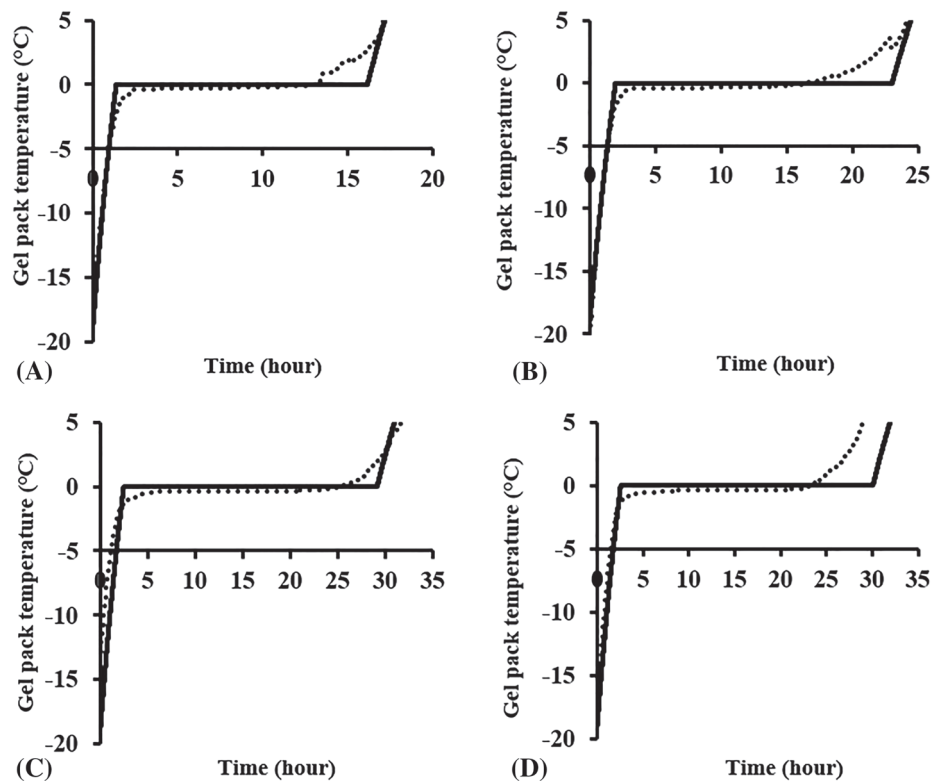


**FIGURE 10** Comparison of calculated (solid line) and measured (dash line) maximum insulation time of packages insulated with, A, EPS; B, EPS with aluminium foil; C, PIR with aluminium foil; D, aerogel with aluminium foil at surrounding temperature of 30°C. AB, aerogel blanket; EPS, expanded polystyrene; PE, polyethylene; PIR, polyisocyanurate

It can be seen that more time is required to raise the product temperature when the total thermal resistance increases. As the calculation of the MIT is partly based on the convolution of Equation 3, the higher thermal resistance leads to faster increase in the MIT. This also means that the effect of different liner materials on their insulating performance will be enlarged as their thickness increases as showed in Figure 9.

Figure 10A–D shows a comparison between the calculated and measured MIT obtained from a package with a liner of EPS, EPS with

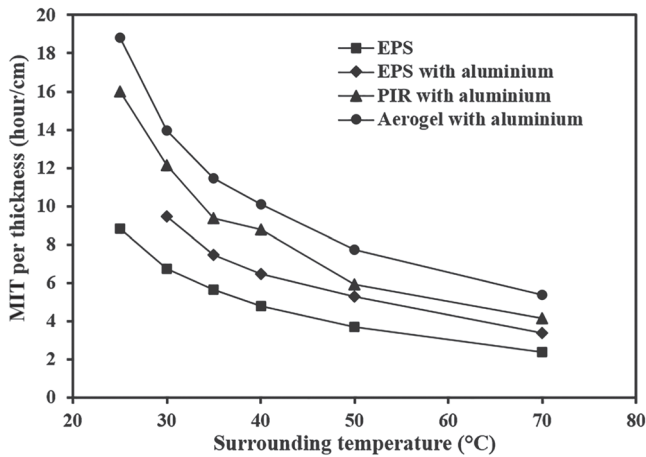


**FIGURE 12** Comparison of measured maximum insulation time per unit thickness at different surrounding temperatures for packages insulated with different materials. EPS, expanded polystyrene; PIR, polyisocyanurate

aluminium foil, PIR with aluminium foil and AB with aluminium foil, respectively, at surrounding temperature of 30°C. For the all cases, the temperature–time behaviour exhibited the three distinct stages described earlier, and there is a good agreement between the modelling and experimental results. In particular, the test results for Stage 1 and large part of Stage 2 are well matched by the theoretical prediction. In contrast, the transition between different stages experiences a sharp turn with the modelling results but is typically smooth for the test results. Such discrepancy is mainly due to the modelling assumption of uniform temperature at any given time. In reality, there should be a non-uniform temperature distribution in thick walls and contained bulk products. As the ice pack temperature was measured by the sensor sandwiched between two ice packs, the measured temperature was likely to be slightly higher than that at the centre of equivalent monolithic ice pack in the model. This may explain why the temperature rise after the phase change appeared sooner from the measurement than the model as shown in Figure 10. However, this did not account for the opposite observation at the beginning of the phase change. Nevertheless, Figure 10 shows a good agreement overall between the tests and the model, and the difference is less than 11%. A large error is found in the Figure 10D for the aerogel-insulated package, and this is probably because the insulation performance of the ABs was somewhat compromised by the potential air gap between two individual blankets.

The comparison of the MIT normalised by the thickness of each liner material is summarised in Figure 11. For the packages with high performance insulation materials such as foiled PIR and AB, an increase of 28% and 47% in the MIT per unit thickness is achieved,

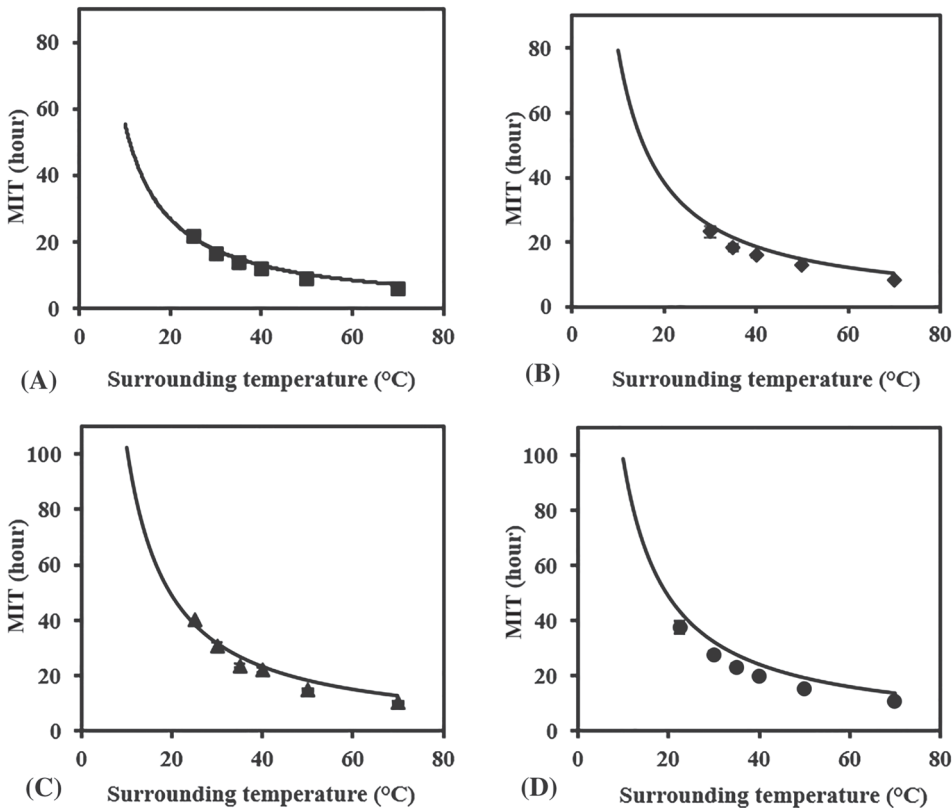


**FIGURE 13** Comparison of calculated (solid line) and measured (markers) maximum insulation time as a function of surrounding temperature for packages insulated with, A, EPS; B, EPS with aluminium foil; C, PIR with aluminium foil; and, D, aerogel with aluminium foil. EPS, expanded polystyrene; PIR, polyisocyanurate



respectively, when compared with the foiled EPS insulated package. Furthermore, an improvement of 79% and 106% in the MIT per unit thickness is obtained for foiled PIR and AB insulated packages compared with the EPS insulated package. It can also be seen from Figure 11 that an excellent agreement between theoretical and experimental results is obtained, although all experimental results have a slightly less MIT than the theoretical prediction meaning that our model tends to marginally underestimate the total heat flux across the package. A satisfactory repeatability of the experimental results is also achieved with maximum standard deviation of 0.7.

#### 4.4 | Effect of surrounding temperature on maximum insulation time

Figure 12 shows the measured MIT per unit thickness of different insulation materials as a function of surrounding temperatures. As expected, an increase in outside temperature resulted in a decrease in the MIT because of higher heat flux entering the package. The temperature dependence of the MIT in Figure 12 follows a logarithmic relation, which is predicted by the government equation for calculating the MIT in Equation 3. This has a significant implication to packaging design for insulating performance as the results from Figure 12 clearly indicate that maintaining a low temperature around an insulated package can bring about significant MIT benefit. This is the case particularly when the package is insulated with high performance insulation materials such as aerogel. In addition, the positive effect of reflective foil on the MIT is found to be sustained over the temperature range as shown in Figure 12. The calculated and measured MIT for packages with different insulation materials are plotted in Figure 13. Once again, an excellent agreement between calculated and measured values can be found over the temperature range investigated in this work.

## 5 | CONCLUSION

Insulating performance of multi-layered wall packages was investigated using experimental measurement and a transient thermal model. The effect on the MIT required for the ice packs to reach 5°C was studied across a range of factors including surface emissivity, insulation thickness, insulation materials and surrounding temperatures. Internal surface with lower emissivity proved to be a very cost-effective approach for improving packaging insulation performance. 46% and 40% increase of the MIT were obtained by applying the aluminium foil to the PE and EPS liners, respectively. Much higher MIT can be achieved by using insulation materials with low thermal conductivity. For instance, 79% and 106% increase in the MIT per unit thickness of insulation liner were obtained by replacing conventional EPS with a foiled PIR board and aerogel blanket. Insulation thickness is another important design factor for packaging performance in passive temperature control as the MIT has a nonlinear relationship with insulation thickness. Similar phenomenon was also observed with

regards to the influence of the surrounding temperature on the MIT. Even with high performance insulation materials, considerable MIT per thickness of insulation can be achieved only when external temperature is maintained around room temperature. The transient thermal model demonstrated the ability to describe three distinctive stages for temperature–time behaviour in insulated packages with coolant. The model was capable of accurately quantifying the contribution from latent heat and sensible heat. Comparison of modelling and experimental results showed an excellent agreement across all the design factors for the packaging insulation performance. As a result, this model can be utilised as a cost-effective tool for packaging design concerning passive temperature control.

#### ACKNOWLEDGEMENT

We would like to express our great gratitude to the Tobermory Fish Company Ltd for their financial support and to the Keysight Technologies for their technical support.

#### ORCID

Liu Yang  <https://orcid.org/0000-0001-8475-1757>

#### REFERENCES

1. Kucharek M, Yang L, Wang K. Assessment of insulating package performance by mathematical modelling. *Packaging Technology and Science*. 2020;33(2):65-73.
2. Changfeng G, Yujie C, Bo L. Numerical simulation and experimental study of the heat transition in a foam container. *Journal of Cellular Plastics*. 2013;50(1):15-36.
3. Burgess G. Practical thermal resistance and ice requirement calculations for insulating packages. *Packaging Technology and Science*. 1999; 12:75-80.
4. Jay S, Sanjiv J, Koushik S. The effect of distribution on product temperature profile in thermally insulated containers for express shipments. *Packaging Technology and Science*. 2012;26:327-338.
5. Choi SJ, Burgess G. Practical mathematical model to predict the performance of insulating packages. *Packaging Technology and Science*. 2007;20(6):369-380.
6. Terpák J, Kukurugya J, Pitoňák M. Simulation model for analysis of thermal processes in thermo-insulating food packaging. Paper presented at: Carpathian Control Conference (ICCC), 2012 13th International 2012.
7. Stubbs D, Pulko S, Wilkinson A. Wrapping strategies for temperature control of chilled foodstuffs during transport. *Transactions of the Institute of Measurement and Control*. 2004;26(1):69-80.
8. Margeirsson B, Lauzon HL, Pálsson H, et al. Temperature fluctuations and quality deterioration of chilled cod (*Gadus morhua*) fillets packaged in different boxes stored on pallets under dynamic temperature conditions. *International Journal of Refrigeration*. 2012;35(1): 187-201.
9. Valtýsdóttir KL, Margeirsson B, Arason S, Pálsson H, Gospavic R, Popov V. Numerical heat transfer modelling for improving thermal protection of fish packaging. Paper presented at: CIGR Section VI International Symposium on Towards a Sustainable Food Chain Food Process, Bioprocessing and Food Quality Management 2011.
10. Xie G, Wang C, Ji T, Sunden B. Investigation on thermal and thermomechanical performances of actively cooled corrugated sandwich structures. *Appl Therm Eng*. 2016;103:660-669.
11. Xie J, Zhang R, Xie G, Manca O. Thermal and thermomechanical performance of actively cooled pyramidal sandwich panels. *International Journal of Thermal Sciences*. 2019;139:118-128.

12. Van Boxtael S, Habib I, Jacxsens L, et al. Food safety issues in fresh produce: bacterial pathogens, viruses and pesticide residues indicated as major concerns by stakeholders in the fresh produce chain. *Food Control*. 2013;32(1):190-197.
13. Echols MA. Food safety regulation in the European Union and the United States: different cultures, different laws. *Colum J Eur L*. 1998; 4:525-545.
14. Xc L, Jy S. Method for measuring object surface emissivity. *Automatic Measurement and Control*. 2007;26(8):48-56.
15. Heaney JB. Efficiency of aluminized mylar insulation at cryogenic temperatures. Paper presented at: Cryogenic Optical Systems and Instruments VIII; 1998.

**How to cite this article:** Wang K, Yang L, Kucharek M. Investigation of the effect of thermal insulation materials on packaging performance. *Packag Technol Sci*. 2020;1-10. <https://doi.org/10.1002/pts.2500>